CELLULAR AUTOMATON MODEL OF PRECIPITATION/DISSOLUTION COUPLED WITH SOLUTE TRANSPORT

T. Karapiperis

Paul Scherrer Institute, CH-5232 Villigen PSI, Switzerland

Abstract

Precipitation/dissolution reactions coupled with solute transport are modelled as a cellular automaton in which solute molecules perform a random walk on a regular lattice and react according to a local probabilistic rule. Stationary solid particles dissolve with a certain probability and, provided solid is already present or the solution is saturated, solute particles have a probability to precipitate. In our simulation of the dissolution of a solid block inside uniformly flowing water we obtain solid precipitation downstream from the original solid edge, in contrast to the standard reaction-transport equations. The observed effect is the result of fluctuations in solute density and diminishes when we average over a larger ensemble. The additional precipitation of solid is accompanied by a substantial reduction in the relatively small solute concentration. The model is appropriate for the study of the rôle of intrinsic fluctuations in the presence of reaction thresholds and can be employed to investigate porosity changes associated with the carbonation of cement.

1 Introduction

Natural phenomena taking place in geological media often involve intricately coupled physical and chemical processes. The dissolution of minerals by flowing groundwater and their precipitation out of saturated solutions play a fundamental rôle in the diagenetic changes of sediments and the weathering of rocks. Precipitation/dissolution reactions can change rock properties (e.g. porosity, sorption capacity) and thereby influence the transport of solutes through the rocks. It is clear that the assessment of natural and engineered geological barriers aimed at containing the migration of soluble contaminants will depend substantially on the coupling between solute-mineral reactions and the water-conducting properties of the solid matrix. The reactions between species in different phases are characterised by spatial and temporal variations in the set of reacting species, while the transfer of matter between the phases results in moving solid boundaries. Depending on the time scales of interest, a kinetic description of heterogeneous chemical reactions may become necessary when the reaction rates are lower than the rates at which mobile reactants are transported to the solid surfaces [1]. Although the problem of modelling such systems can be addressed in principle in the framework of coupled non-linear partial differential equations (PDE's), the numerical task is usually so complex (the numerical algorithm has to be continually readjusted to a varying set of reactions and boundaries) that drastic approximations become indispensable in practice [2]. With a view to overcome at least some of the difficulties, we propose to model heterogeneous reactions coupled with mass transport as a *cellular automaton (CA)*, taking advantage of the local and parallel character of the natural processes.

The model described here continues and enriches the cellular automaton model of coupled chemical reactions and mass transport that was presented in Ref. [3]. In that case, the time evolution of

single-phase systems involving particle transport (advection and diffusion/dispersion) coupled with arbitrary chemical reactions was modelled by synchronous application, in regular time intervals, of a local probabilistic rule to all sites of a regular spatial lattice spanning the extent of the physical system of interest. The model was versatile enough to describe a variety of physical phenomena ranging from fluctuation-dominated behaviour in the annihilation reaction $a + b \rightarrow nothing$ to pattern formation with complex autocatalytic reaction schemes [3]. The model was found capable of approximating the solution of PDE's, while being able to account for microscopic effects that are typically washed out by the averaging procedure that leads to the macroscopic equations. It should be clear, however, that we do not aim at a strictly *microscopic* description of physical phenomena and the 'particles' in our simulations do not correspond to individual molecules of the actual system. Accounting for such inessential and hardly comprehensible detail would amount to an enormous waste of resources. Instead, our *mesoscopic* approach accounts for those elements of microscopic reality (e.g. statistical fluctuations) that are likely to play a rôle at the macroscopic level; it further models physicochemical processes at a sufficiently elementary level to make the implementation of various reaction schemes and boundary conditions, as well as their local readjustment as the system evolves, intuitively transparent.

When it comes to numerical implementation, the algorithms obtained in our approach iterate an integer field (numbers of particles), which is free of round-off errors, with real numbers appearing only in the form of bounded probabilities. As a result, these algorithms are inherently stable. By contrast, given the highly non-linear nature of the problems we wish to solve, the stability of the respective finite difference equations (FDE's) would have to be tediously established on a case by case basis. At the same time, however, the large size of the ensembles that have to be simulated in order to achieve good statistics tends to slow down CA simulations. Thus, it became clear from the applications to single-phase systems that, for simple boundary conditions and physicochemical parameters invariant in space and time, conventional numerical techniques (e.g. FDE's) are computationally more efficient than CA simulations. In such cases conventional methods for the solution of the macroscopic equations are sufficient, unless they either suffer from intractable stability problems or the impact of microscopic effects at the macroscopic level cannot be neglected. Of course CA algorithms map naturally onto the architecture of massively parallel computers, which are still in an early stage of their development. We believe that future computer designs will allow us to perform parallel simulations of large ensembles much more efficiently and to thus better utilise the potential of CA algorithms.

The situation is, however, different in the presence of heterogeneous reactions. Precipitation or dissolution can only occur if solid is already present or the solution is saturated. The existence of thresholds for the onset of the reactions implies that the set of reactants may vary in space and time, depending on whether certain minerals are reacting or not. Since the removal or addition of solid changes the boundaries of the conducting channels, transport properties are further closely coupled with reaction kinetics and may vary in space and time. We believe CA modelling to be well-suited for modelling heterogeneous reactions coupled with mass transport. A CA model can account for spatial variations in flow and reaction parameters at no additional cost and, by modelling processes at an elementary level, it is capable of readjusting locally their characteristics as they vary in the process

of the simulation. The mesoscopic approach can be applied to solute-mineral reactions at different spatial scales. On the one hand, one can address the problem at pore level [4], by modelling the flow of water through the actual pores and deriving explicitly the time evolution of porosity and permeability. Alternatively, one can model the system at a laboratory or field scale, assuming a phenomenological relation between the amount of precipitated or dissolved solid and the associated porosity changes. In the latter case, which is the point of view represented in this paper, one exploits the ease with which a CA models processes with characteristics varying in space and time. These two levels of modelling are to be seen as complementary, the simulations at pore scale delivering the fundamental justification for the phenomenological relations assumed at the larger scale.

This paper is organised as follows: The model is introduced in the following section and numerical simulations are presented and discussed in a subsequent section. Some theoretical questions are raised and future applications of the model are proposed in a final section.

2   Model of precipitation/dissolution

In our model physical and chemical processes take place on a regular spatial lattice of spacing λ, according to a local rule applied synchronously to all sites in regular time intervals τ. The transport of solutes is modelled as a random walk, whereby particles move to neighbouring sites or remain at their present site with prescribed probabilities. The macroscopic manifestation of the random walk is a combination of *advection* and *diffusion*. The displacement probabilities are chosen so that the desired *advection velocity* V and *diffusion coefficient* D are obtained in the continuum limit ($\lambda \to 0$ and $\tau \to 0$) [1]. Considering, for the sake of simplicity, a one-dimensional system, we define the probabilities that a particle of solute s_α moves to the next site on the right (p_α) or the left (q_α) so that

$$V_\alpha \equiv (p_\alpha - q_\alpha)\frac{\lambda}{\tau} \qquad , \qquad D_\alpha \equiv (p_\alpha + q_\alpha)\frac{\lambda^2}{2\tau} \quad . \tag{2.1}$$

In Eq. (2.1), V and D are assigned a species label so that species with different transport properties can be modelled on the same lattice by choosing p_α and q_α individually for each species. When taking the continuum limit, we also let $p_\alpha - q_\alpha \to 0$ and we keep $\lambda^2/2\tau$ and $(p_\alpha - q_\alpha)\lambda/\tau$ finite. Spatially varying V_α and D_α can be treated by making p_α and q_α position dependent; defining V_α and D_α as above, we then identify the advection velocity with $W_\alpha(x) \equiv V_\alpha(x) - dD_\alpha(x)/dx$.

Ref. [3] contains a thorough discussion of our model of chemical reactions among solutes. Here we summarise the points that are relevant for the extension to heterogeneous reactions. In solution we allow arbitrary reactions of the type

$$\sum_\alpha \nu_\alpha s_\alpha \overset{K_1}{\underset{K_2}{\rightleftharpoons}} \sum_\alpha \mu_\alpha s_\alpha \quad , \tag{2.2}$$

where K_1, K_2 are the *rate constants* and the *stoichiometric coefficients* ν_α, μ_α are non-negative integers. Referring for brevity to a typical lattice site located at x as 'site x', we define the *occupation*

---

[1]We assume that *mechanical dispersion* can be macroscopically described by an effective diffusion term, so 'diffusion' should be understood in a broader sense than just *molecular diffusion*.

number $N_\alpha(x,t)$ as the number of particles of species s_α that are to be found on site x, at time t. The action of the chemical reaction operator $\mathcal{C}$ on $N_\alpha(x,t)$ is defined by the equation

$$\mathcal{C}N_\alpha(x,t) = N_\alpha(x,t) + \sum_{r=1}^{R} \left(\nu_{\alpha r}^{(f)} - \nu_{\alpha r}^{(i)} \right) \eta_{x,r} \quad , \tag{2.3}$$

where $\eta_{x,r}$ is a random Boolean variable and $\nu_{\alpha r}^{(f)}$ and $\nu_{\alpha r}^{(i)}$ are stoichiometric coefficients referring to products and reactants, respectively. The summation runs over all R one-way reactions obtained by separating the forward from the reverse process (irreversible reactions are added to the list as they are). Reaction r takes place when $\eta_{x,r} = 1$, which happens with probability

$$\wp(\eta_{x,r} = 1|\{N_\beta(x,t) : s_\beta \in \mathcal{S}\}) \equiv P_r F_r \left(\{N_\beta(x,t) : s_\beta \in \mathcal{S}\} \right) \quad , \tag{2.4}$$

where P_r is a real constant, F_r is a function of the occupation numbers and $\mathcal{S}$ is the set of all species in solution. According to chemical reaction rule II of Ref. [3],

$$F_r \left(\{N_\beta(x,t) : s_\beta \in \mathcal{S}\} \right) = \prod_\beta \prod_{m=1}^{\nu_{\beta r}^{(i)}} (N_\beta(x,t) - m + 1) \quad . \tag{2.5}$$

For example, if r is the reaction $a + b \rightarrow c$, then it occurs with probability $P_r N_a N_b$. In deriving the continuum limit of the full model we also take $P_r \rightarrow 0$, keeping P_r/τ finite. Of course, care has to be taken so that the probability defined by Eqs. (2.4) and (2.5) does not exceed 1. It is always possible to ensure this by choosing P_r sufficiently small (so that $P_r N_a N_b \leq 1$, $\forall x, t$ in the above example), since the occupation number remains finite during a simulation.

The particle density $\rho_\alpha(x,t)$ is defined by averaging the occupation number $N_\alpha(x,t)$ over an ensemble of macroscopically identical systems. In Ref. [3] it is shown how rule (2.5) leads, under the assumptions of *molecular chaos* (no correlations between the occupation numbers of different species) and a smooth particle density function, to the standard rate law, which is consistent with the *law of mass action* at equilibrium. The rate constant k_r is given by

$$k_r \equiv \frac{P_r}{\tau} \quad . \tag{2.6}$$

Thus, for the reaction $a + b \rightarrow c$ we obtain a rate of $k_r \rho_a \rho_b$.

The novel element in solute-mineral reactions consists in the existence of a precipitation threshold: solid must already be present or the solution must be saturated before the reaction may proceed. We investigate the simple precipitation/dissolution reaction

$$\mathcal{M}(s) \underset{K_2}{\overset{K_1}{\rightleftharpoons}} a + b \quad , \tag{2.7}$$

where a, b are aqueous species, $\mathcal{M}$ is a solid and K_1, K_2 are the rate constants. We assume $\mathcal{M}$ to be a mineral occupying a section of an otherwise inert rock of uniform porosity ϵ. Water flows through the rock and gradually dissolves the mineral according to the forward reaction in (2.7). The solutes produced are then transported by advection, mechanical dispersion and molecular diffusion; in the

4

process they may recombine and precipitate according to the reverse reaction in (2.7). In this paper we treat the porosity as a constant, making sure that the amount of dissolved and reprecipitated mineral is small enough to make a readjustment of the porosity unnecessary. This is clearly a restriction that we can easily relax when we address the question of porosity changes caused by solute-mineral reactions. At this stage, however, a variable porosity would unnecessarily complicate our effort to compare our model to the standard macroscopic approach.

The macroscopic reaction-transport equations for the system considered here are

$$\epsilon \frac{\partial C_a(x,t)}{\partial t} = -\epsilon V_a \frac{\partial C_a(x,t)}{\partial x} + \epsilon D_a \frac{\partial^2 C_a(x,t)}{\partial x^2} + \zeta(x,t)\left(K_1 - \epsilon^2 K_2 C_a(x,t) C_b(x,t)\right)$$
$$\frac{\partial C_{\mathcal{M}}(x,t)}{\partial t} = -\zeta(x,t)\left(K_1 - \epsilon^2 K_2 C_a(x,t) C_b(x,t)\right) \quad,$$
(2.8)

where C_a and C_b are the concentrations of the solutes in mol per m^3 of water and $C_{\mathcal{M}}$ is the 'concentration' of solid in mol per m^3 of rock. ζ takes the value 0 or 1 according to

$$\zeta(x,t) = \begin{array}{ll} 1\,, & \text{if } C_{\mathcal{M}}(x,t) > 0 \text{ or } C_a(x,t) C_b(x,t) > \mathcal{K} \\ 0\,, & \text{otherwise} \end{array} \quad,$$
(2.9)

where $\mathcal{K} \equiv K_1/\epsilon^2 K_2$ is the *solubility product*. The equation for C_b is analogous to the one for C_a.

We model the transport of the mobile species a and b as a random walk on a lattice, as explained in the beginning of this section. The transport operation leaves $\mathcal{M}$-particles unaffected. After the transport operation has been applied synchronously to the entire lattice, the evolution of the system from time t to $t + \tau$ is completed by application of the chemical reaction operation. The local rule for the reaction (2.7) is defined in terms of two constants, P_1 and P_2, and two random Boolean variables, $\eta_{x,1}$ and $\eta_{x,2}$. $\eta_{x,1} = 1$ ($\eta_{x,2} = 1$) signals the occurrence of a dissolution (precipitation) event at x.

In dissolution, solid $\mathcal{M}$-particles are converted to solute a- and b-particles. Dissolution is of course possible at a site x if one or more $\mathcal{M}$-particles are present there. If this condition is fulfilled, then we choose $\eta_{x,1} = 1$ with probability P_1, which is independent of the amount of solid available. If $\eta_{x,1} = 1$, the number of $\mathcal{M}$-particles at x is diminished by 1, while those of a- and b-particles are increased by 1. At most one $\mathcal{M}$-particle may dissolve per site during an evolution step from t to $t + \tau$.

Precipitation results in the replacement of solute a- and b-particles by solid $\mathcal{M}$-particles. The process is possible at a site x if at least one $\mathcal{M}$-particle is already present there or if the product of the densities of a and b (calculated as ensemble averages of the respective occupation numbers N_a and N_b) is greater than P_1/P_2. In the former case precipitation occurs around a nucleus of already present solid, whereas the latter inequality amounts to the saturation condition of the solution. If at least one of these conditions is fulfilled, then we choose $\eta_{x,2} = 1$ with probability $P_2 N_a N_b$. We note that the saturation condition is the same for the entire ensemble, whereas the reaction probability is defined individually for each member. The probability of precipitation is naturally higher the greater the number of solute particles present and vanishes when either or both species are absent. If $\eta_{x,2} = 1$, the number of $\mathcal{M}$-particles at x is increased by 1, while those of a- and b-particles are diminished by 1. At most one a- and one b-particle may be subtracted per site during an evolution step. The definition of the reaction probability for precipitation guarantees that there is a sufficient amount of solute particles when the reaction proceeds.

Referring to the forward and backward reactions in (2.7) as reactions 1 and 2, respectively, we write the probability of their occurrence as

$$\wp(\eta_{x,1} = 1) \equiv P_1 \theta\left(N_{\mathcal{M}}(x,t)\right) \ , \tag{2.10a}$$

$$\wp(\eta_{x,2} = 1) \equiv P_2 N_a(x,t) N_b(x,t) \left[\theta\left(N_{\mathcal{M}}(x,t)\right) + \delta_{N_{\mathcal{M}}(x,t),0} \ \theta\left(\rho_a(x,t)\rho_b(x,t) - \frac{P_1}{P_2}\right)\right] \ . \tag{2.10b}$$

We define $\rho_\alpha(x,t) \equiv\ <N_\alpha(x,t)>$, where $<\ldots>$ denotes an ensemble average. The value of the θ-function $\theta(z)$ is 1 if $z > 0$ and 0 otherwise. $\delta_{i,j} = 1$ or 0 according as the integers i and j are equal or not.

Assuming no correlations between a-, b- and $\mathcal{M}$-particles (molecular chaos), we obtain the reaction rate

$$\frac{\partial \rho_{\mathcal{M}}(x,t)}{\partial t} = -\frac{P_1}{\tau} \wp\left(N_{\mathcal{M}}(x,t) > 0\right) + \frac{P_2}{\tau} \rho_a(x,t)\rho_b(x,t) \cdot$$
$$\left[\wp\left(N_{\mathcal{M}}(x,t) > 0\right) + \wp\left(N_{\mathcal{M}}(x,t) = 0\right) \ \wp\left(\rho_a(x,t)\rho_b(x,t) > \frac{P_1}{P_2}\right)\right] \ . \tag{2.11}$$

The same term, but with opposite sign, appears on the RHS of the reaction-transport equations derived in the continuum limit for a and b. $\wp\left(N_{\mathcal{M}}(x,t) = 0\right)$ denotes the probability that there are no solid particles at the given location and time, and $\wp\left(N_\alpha(x,t) > 0\right) = 1 - \wp\left(N_\alpha(x,t) = 0\right)$. $\wp\left(\rho_a(x,t)\rho_b(x,t) > P_1/P_2\right)$ is the probability that the saturation condition is fulfilled. For a given spatially smooth density $\rho_\alpha(x,t)$ of particles we expect these probabilities to depend on the macroscopic parameters of the system. Thus, for *randomly moving* particles, such as the solutes in our model, the occupation numbers obey the Poisson distribution $\wp\left(N_\alpha(x,t) = n\right) = e^{-\rho_\alpha(x,t)}\rho_\alpha^n(x,t)/n!, \ n \geq 0$. As we shall see in the next section, this is not true about the immobile solid particles.

The transition from particle densities to concentrations is made by the relations $C_a = \gamma\rho_a$, $C_b = \gamma\rho_b$ and $C_{\mathcal{M}} = \gamma\epsilon\rho_{\mathcal{M}}$, where the constant γ can be fixed by relating the initial concentrations of the physical problem to the initial particle densities of the simulation. The macroscopic equations obtained from our mesoscopic model differ from Eqs. (2.8) in the precise definition of the switch that signals the onset of precipitation/dissolution, but this difference is only likely to play a rôle for very small solid particle densities. Comparing with (2.8), we are led to relate the rate constants to the reaction parameters used in the simulation by $K_1 = \gamma\epsilon P_1/\tau$ and $K_2 = P_2/\gamma\epsilon\tau$.

3   Simulations of precipitation/dissolution

We have applied the CA model described in the previous section to systems with one-dimensional geometry, assuming translational invariance in the other two dimensions. In this section we compare the results of our simulations with the solution of the macroscopic reaction-transport equations.

We consider first the dissolution of a small amount of solid ($\epsilon \simeq 1$) placed at $t = 0$ in a stream of uniformly flowing water. Solid and solute particles reside on a one-dimensional lattice of $\mathcal{N}_x = 101$ sites and spacing λ. The water is not explicitly modelled. Initially we place randomly 510 particles of the solid $\mathcal{M}$ on the left half of the otherwise empty lattice, to an average density of 10 particles/site. The solid particles do not move. Solid can, however, be transferred across the lattice indirectly by

dissolution, transport of the solutes and reprecipitation. At each site where solid is present there is a probability of $P_1 = 0.04$ that a solid particle dissolves during an update. Dissolution amounts to disappearance of an $\mathcal{M}$-particle and creation of one a- and one b-particle in solution. The solutes a and b are carried along by flowing water with an advection velocity of $V_a = V_b = 0.1\,\lambda/\tau$ (i.e. it would take a solute particle 1000 updates, applied in time intervals of τ, to traverse the lattice by advection alone) from left to right. The solutes are additionally subject to diffusion/dispersion with a diffusion coefficient of $D_a = D_b = \lambda^2/2\tau$. In the simulation, solute particles perform a random walk with displacement probabilities of $p_a = p_b = 0.55$ to the right and $q_a = q_b = 0.45$ to the left. At every time step we evaluate the particle densities $\rho_a(x,t)$ and $\rho_b(x,t)$ by averaging the particle numbers $N_a(x,t)$ and $N_b(x,t)$ over an ensemble of $\mathcal{N}_y$ systems. One can think of the ensemble members as being aligned in a y-direction orthogonal to the actual x-direction of the system; then the averaging is performed over y, for fixed x and t. Defining the parameter $P_2 = 0.4$, we specify that precipitation may take place only if $N_\mathcal{M}(x,t) > 0$ or $\rho_a(x,t)\rho_b(x,t) > P_1/P_2$. Once allowed, precipitation, i.e. the reverse of the dissolution process described above, proceeds with probability $P_2 N_a(x,t) N_b(x,t)$.

Solute particles are subject to the following boundary conditions: The boundary site on the left ($x = 0$) is a sink absorbing all a- or b-particles that reach it. At the right boundary, $x = L \equiv (\mathcal{N}_x - 1)\lambda$, we impose the macroscopic boundary condition $\partial\rho_a(x,t)/\partial x|_{x=L} = \partial\rho_b(x,t)/\partial x|_{x=L} = 0$. Equivalently, we set the diffusive flux, which is proportional to the density gradient, equal to zero at $x = L$; this leaves only advection to take care of net solute transport across the boundary. To implement the zero-gradient boundary condition in our model we follow Ref. [3]: the lattice is formally extended by one lattice spacing; before each transport operation the occupation number of the new site ($x = L + \lambda$) is set equal to that of the site immediately preceding the boundary ($x = L - \lambda$). As long as the particle density is not the same at L and $L - \lambda$, a net amount of particles will diffuse either from L to $L - \lambda$ and $L + \lambda$ or vice versa until there is no density gradient at the boundary. In physical terms, we superpose equal and opposite amounts of outgoing and incoming diffusive flux and thus make the total diffusive flux vanish.

Fig. 1 displays the profile of solid particle density obtained from the above simulation after $\mathcal{N}_t = 5000$ iterations. The solid, dashed and dotted curves show the results obtained from three different simulations with ensemble sizes $\mathcal{N}_y = 250$, 1000 and 4000, respectively. The dot-dashed curve shows the result of the macroscopic transport equations (obtained from (2.8) by setting ϵ, γ, λ and τ equal to unity). We see that a large fraction of the original solid has dissolved. In the simulations, solid reprecipitates downstream from the original solid edge, in contrast to the macroscopic description where the edge remains sharp. The observed effect is entirely due to statistical fluctuations in the solute densities: due to fluctuations, the product of the densities occasionally exceeds the solubility limit and precipitation ensues. Fig. 1 shows that averaging over a larger ensemble reduces the fluctuations and the resulting precipitation.

The difference between the simulations and the macroscopic equations on the left side of the solid block is of different origin:

(i) It does not depend on the size of the ensemble and is therefore not of statistical origin.

Figure 1: Density profile of solid particles. The meaning of the different curves is explained in the text.

(ii) It depends weakly on the number of transport steps per reaction step, n_D. Increasing n_D washes out reaction correlations between a- and b-particles; in Ref. [3], such correlations were found to influence the macroscopic properties of a system of diffusing a-, b- and c-particles subject to the reaction $a + b \rightleftharpoons c$; it was also found that correlations were practically eliminated for $n_D = 10$ (e.g. the remaining effect on the equilibrium reaction quotient $\rho_c/\rho_a\rho_b$ was less than 0.3% for a homogeneous system). For the precipitation/dissolution reaction we find that increasing n_D from 1 to 4 (while keeping V_α and D_α fixed by appropriate readjustment of p_α and q_α) reduces the solid particle density by 20 - 30 % in the middle of the upstream tail of the density profile, but increasing n_D further to 9 makes only a 2 - 3 % difference.

(iii) It diminishes systematically as we approach the continuum limit by refining the discretisation of the lattice (i.e. increasing $\mathcal{N}_x$ while keeping macroscopic parameters fixed by appropriate readjustment of $\mathcal{N}_t$, p_α, q_α and P_r). We have confirmed this for $\mathcal{N}_x = 200$ and 400, but were prevented from implementing larger lattices by CPU time limitations. It is worth noting that the amount of solid precipitating downstream is left unaffected (within fluctuations) by the refined discretisation for given ensemble size.

We next look at a cross-section of the ensemble of systems along the fictitious y-direction: for given x and t, there is an interesting difference between the distributions of solute and solid occupation numbers within the ensemble. For the solutes a and b, occupation numbers are distributed, within the statistics of the ensemble, according to the Poisson distribution consistent with the average density. This is expected due to the randomising action of the motion of these particles. Since solid particles are placed randomly, as described above, their initial distribution is also Poisson [2]. The initial distribution

---

[2]The macroscopic fate of the system would be the same if exactly 10 solid particles were placed at every site initially.

Figure 2: Distribution of solid-particle occupation numbers at $x = 40\lambda$ and (a) $t = 0$, (b) $t = 5000\tau$. The meaning of the different symbols and curves is explained in the text.

of occupation numbers at $x = 40\lambda$ is shown in Fig. 2a for the three simulations considered in Fig. 1 (solid circles, open circles and crosses, respectively); for comparison, the solid, dashed and dotted curves show the Poisson distributions for the respective particle densities. A similar plot at time $t = 5000\tau$ (Fig. 2b) reveals a much wider distribution of occupation numbers. In this case we observe a remarkably high frequency of sites with no solid particles. This is related to the small initial particle density. In simulations with 10 and 100 times higher initial densities, the frequency of empty sites is very small ($\sim 1\%$) and negligible respectively, but occupation numbers still follow broad distributions.

In order to appreciate the implications of density fluctuations for models of the dissolution of actual minerals, we consider now a piece of rock of length $L = 10m$, with a uniform porosity of $\epsilon = 11\%$. The left half of the rock is occupied at time $t = 0$ by a soluble mineral with a density of 2.71 g/cm^3 and a molecular weight of 100. The rate constants for dissolution and precipitation are $K_1 = 1.2 \times 10^{-9} mol \; m^{-3} s^{-1}$ and $K_2 = 3.3 \times 10^{-5} m^3 mol^{-1} s^{-1}$, respectively. Thus, the solubility product is $\mathcal{K} = 10^{-2.5} mol^2 m^{-6} = 10^{-8.5} (mol/\ell)^2$. The physical and (equilibrium) chemical parameters are chosen to be consistent with calcite ($CaCO_3$) as a typical mineral in the geological systems of interest. The dissolved species Ca^{2+} and CO_3^{2-} move with an advection velocity of $10^{-8} m/s$ and a diffusion coefficient of $10^{-9} m^2/s$.

For the simulation we choose $\lambda = 10^{-2} m$, $\tau = 5 \times 10^4 s$ and $\gamma = 0.28 \, mol/m^3$. At time $t = 10^{10} s$ a small fraction of the solid has been depleted from the left side of the original block of mineral (Fig 3a). The simulation agrees well with the result of the macroscopic equations (2.8); the remaining small discrepancy is qualitatively reminiscent of the relatively larger one observed in Fig. 1. Solid precipitates downstream from the original solid edge, an effect which is absent from

Figure 3a: Profile of solid 'concentration' (solid line: simulation, dotted line: macroscopic equations).

Figure 3b: Concentration profiles of solute (horizontal dotted line and solid line running on the average parallel to it: macroscopic equations and simulation, respectively; dashed line is a smoothed version of solid line; axis labelled on the right) and solid (vertical dotted curve and solid line running partly parallel to it: macroscopic equations and simulation, respectively; axis labelled on the left).

the result of the macroscopic equations (Fig 3b). The amount of precipitating solid diminishes as the size of the ensemble increases (not shown in the figure, which was obtained with $\mathcal{N}_y = 200$), pointing, as already remarked in connection with Fig. 1, to the crucial rôle of statistical fluctuations. The amount of solid that is found downstream from the edge is tiny on the scale of the total amount of solid, but the consequences can be more serious for the concentration of solutes. The net precipitation of solid in the right half of the lattice is accompanied by a reduction in solute concentration relative to the prediction of the macroscopic equations. In Figs. 3a and 3b, of 400 million solid particles initially present, about 4500 have been removed from the solid block and about 500 have precipitated in the right half of the lattice. This suffices, however, to produce a 20-25 % suppression in solute concentration, as a comparison of the dotted and dashed curves shows. The importance of this suppression will depend of course on the particular situation, but it illustrates the fact that corrections to reaction rates can have a very different impact on species whose concentrations differ by several orders of magnitude (5-6 in the case at hand). The size of the effect on the spatial distribution of the mineral itself is likely to become significant at sufficiently long times. When the time scale is long enough for precipitation/dissolution to cause changes in the porosity, statistical fluctuations in solute concentrations will certainly influence those changes, to a degree, however, that remains to be investigated.

4   Discussion and outlook

The mesoscopic model of precipitation/dissolution introduced here is seen as part of a comprehensive model of the coupled transport and chemical reactions of solutes in geological media. As in the model of transport and reactions in single-phase systems presented in Ref. [3], physical and chemical processes are modelled as simple CA rules applied to a collection of particles on a regular lattice. One can thus model spatial and temporal variations in the characteristics of the system by local readjustment of parameters without changing the overall algorithm. This, coupled with the guaranteed stability of our algorithms, provides a significant advantage over standard numerical methods when modelling heterogeneous reactions. Solute-mineral reactions have the distinctive feature that they become possible only beyond a certain threshold, so that the set of reactions itself and the boundaries between different phases may vary in space and time. Our model provides further a natural way to study the rôle of fluctuations in coupled physicochemical processes. We have seen one distinctive consequence of statistical fluctuations in solute concentrations in the form of mineral precipitation beyond solid edges that would remain sharp according to the standard macroscopic equations. This has a significant effect on the relatively (compared to the mineral) small concentrations of solutes, but it may also influence the porosity of the solid matrix.

Since the particles of our simulations do not model individual molecules of the actual system, the interpretation of statistical fluctuations and their consequences is not immediately obvious. We assume here a phenomenological point of view, allowing for microscopic processes not explicitly accounted for in our model to contribute to the fluctuations we model. Then one has to fix the amplitudes of the fluctuations by comparing the size of the resulting effects with real systems. From a theoretical point of view our model of precipitation/dissolution can be seen as a paradigm of a reaction-transport

system subject to reaction thresholds. It would be interesting to develop the corresponding stochastic differential equations with the appropriate noise amplitude and compare their results with those of our simulations. One could thus study in a qualitatively different framework the rôle of intrinsic noise along the lines of the work reported in Ref. [5].

In our simulations so far we have modelled the transport of solutes assuming that their advection follows a given velocity field. If the solute concentration is small enough, the velocity field coincides with that of pure water flowing under the given mechanical conditions. The dynamics of water flow is governed by the Navier-Stokes equations, which for a porous medium go over to Darcy's law on a macroscopic scale. The problem of solute transport can be solved by a two-step process, where one first solves the appropriate hydrodynamic equations (by CA or other numerical methods) and then uses the resulting velocity field as an input parameter to the equations of motion of the solute. It may, however, be more economical to model the motion of the solute directly by incorporating a random walk in the evolution rule of a *lattice gas*, i.e. one of the CA used for the simulation of fluid dynamics [6]. Chemical reactions can be added and the full algorithm is iterated in time taking into account possible changes in the mechanical properties of the solid matrix due to the reactions.

The development of our CA model for precipitation/dissolution was motivated largely by its intended application to the investigation of the evolution of porosity as a result of solute-mineral reactions. A simple system which possesses the necessary ingredients for such an investigation consists of a block of cement $(Ca(OH)_2)$ dissolving in the presence of CO_3^{2-} (e.g. through contact with atmospheric air) and reprecipitating as $CaCO_3$. A simple model of the carbonation of cement appeared previously in Ref. [7]. The chemistry of the system can be schematically represented by the reactions

$$Ca(OH)_2 \; \rightleftharpoons \; Ca^{2+} + 2\,OH^-$$
$$CaCO_3 \; \rightleftharpoons \; Ca^{2+} + CO_3^{2-} \quad .$$
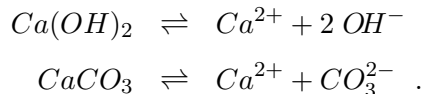
Significant porosity changes by $CaCO_3$ precipitation have been observed experimentally [8]. They can be crucial, for example, in the assessment of cement as a barrier to the migration of soluble contaminants released following a failure in a waste repository. Our approach offers the possibility of developing flexible models of heterogeneous reactions coupled with mass transport and reactions in the aqueous phase. Applications to real geological systems will help us appreciate better the rôle of intrinsic fluctuations. By developing in parallel the corresponding stochastic differential equations and comparing them with mesoscopic simulations, we can test to what extent the full detail of the latter can be effectively grasped in an more economical modelling framework. The relative computational efficiency of the different approaches will depend largely on the specific applications, as well as on future developments in massively parallel architectures and hardware.

Acknowledgements

References

[1] R. Wollast, in *Aquatic Chemical Kinetics*, W. Stumm, ed. (Wiley, New York, 1990), pp. 431–445.

[2] P. C. Lichtner, Geochim. Cosmochim. Acta **52**(1988)143.

[3] T. Karapiperis and B. Blankleider, Physica **D 78**(1994)30.

[4] J. T. Wells, D. R. Janecky and B. J. Travis, Physica **D 47**(1991)115.

[5] J. R. Weimar, D. Dab, J.-B. Boon and S. Succi, Europhys. Lett. **20**(1992)627.

[6] G. Doolen, U. Frisch, B. Hasslacher, S. Orszag and S. Wolfram, eds., *Lattice Gas Methods for Partial Differential Equations*, Santa Fe Institute Studies in the Science of Complexity (Addison–Wesley, 1990).

[7] L. M. Brieger and E. Bonomi, J. Comp. Phys. **94**(1991)467.

[8] F.-A. Sarott, M. H. Bradbury, P. Pandolfo and P. Spieler, Cement and Concrete Research **22**(1992)439.